EUROPEAN ORGANIZATION FOR NUCLEAR RESEARCH
Laboratory for Particle Physics

Departmental Report   **CERN/AT 2007-1**

AN INTRODUCTION TO CRYOGENICS

Ph. Lebrun

President, Commission A1 "Cryophysics and Cryoengineering" of the IIR
Accelerator Technology Department, CERN, Geneva, Switzerland

CONTENTS

AN INTRODUCTION TO CRYOGENICS

Ph. Lebrun
President, Commission A1 "Cryophysics and Cryoengineering" of the IIR
Accelerator Technology Department, CERN, Geneva, Switzerland

Abstract

This paper aims at introducing cryogenics to non-specialists. It is not a cryogenics course, for which there exists several excellent textbooks mentioned in the bibliography. Rather, it tries to convey in a synthetic form the essential features of cryogenic engineering and to raise awareness on key design and construction issues of cryogenic devices and systems. The presentation of basic processes, implementation techniques and typical values for physical and engineering parameters is illustrated by applications to helium cryogenics.

1. LOW TEMPERATURES IN SCIENCE AND TECHNOLOGY

Cryogenics is defined as *that branch of physics which deals with the production of very low temperatures and their effect on matter* [1], a formulation which addresses both aspects of attaining low temperatures which do not naturally occur on Earth, and of using them for the study of nature or the human industry. In a more operational way [2], it is also defined as *the science and technology of temperatures below 120 K*. The reason for this latter definition can be understood by examining characteristic temperatures of cryogenic fluids (Table 1): the limit temperature of 120 K comprehensively includes the normal boiling points of the main atmospheric gases, as well as of methane which constitutes the principal component of natural gas. Today, liquid natural gas (LNG) represents one of the largest – and fast-growing – industrial domains of application of cryogenics (Figure 1), together with the liquefaction and separation of air gases (Figure 2). The densification by condensation, and separation by distillation of gases was historically – and remains today - the main driving force for the cryogenic industry, exemplified not only by liquid oxygen and nitrogen used in chemical and metallurgical processes, but also by the cryogenic liquid propellants of rocket engines (Figure 3) and the proposed use of hydrogen as a "clean" energy vector in transportation (Figure 4).

Table 1
Characteristic temperatures of cryogenic fluids [K]

Cryogen	Triple point	Normal boiling point	Critical point
Methane	90.7	111.6	190.5
Oxygen	54.4	90.2	154.6
Argon	83.8	87.3	150.9
Nitrogen	63.1	77.3	126.2
Neon	24.6	27.1	44.4
Hydrogen	13.8	20.4	33.2
Helium	2.2*	4.2	5.2

∗ λ point

Figure 1 130 000 m³ LNG carrier with integrated Invar® tanks (source Gaztransport)

Figure 2 Cryogenic air separation plant with heat exchanger and distillation column towers (source Air Products)

<table>
<tr><td align="center">a) Ariane 5
(25 t liquid hydrogen, 130 t liquid oxygen)</td><td align="center">b) Space Shuttle
(100 t liquid hydrogen, 600 t liquid oxygen)</td></tr>
</table>

Figure 3 Rockets using cryogenic liquid propellants

Figure 4 Automotive liquid hydrogen fuel tank

The quest for low temperatures however finds its origin in early thermodynamics, with Amontons's gas pressure thermometer (1703) opening the way for the concept of absolute zero inferred a century later by Charles and Gay-Lussac, and eventually formulated by Kelvin. It is however with the advent of Boltzmann's statistical thermodynamics in the late nineteenth century that temperature – until then a phenomenological quantity - could be explained in terms of microscopic structure and dynamics. Consider a thermodynamic system in a macrostate which can be obtained by a multiplicity W of microstates. The entropy S of the system was postulated by Boltzmann as

$$S = k_B \ln W \tag{1}$$

with $k_B \simeq 1.38 \ 10^{-23}$ J/K. This formula, which founded statistical thermodynamics, is displayed on Boltzmann's grave in Vienna (Figure 5).

Figure 5 L. Boltzmann's grave in the Zentralfriedhof, Vienna, bearing the entropy formula

Adding reversibly heat dQ to the system produces a change of its entropy dS, with a proportionality factor T which is precisely temperature

$$T = \frac{dQ}{dS} \qquad (2)$$

Thus a low-temperature system can be defined as one to which a minute addition of heat produces a large change in entropy, i.e. a large change in its range of possible microscopic configurations.

Boltzmann also found that the average thermal energy of a particle in a system in equilibrium at temperature T is

$$E \sim k_B T \qquad (3)$$

Consequently, a temperature of 1 K is equivalent to a thermal energy of 10^{-4} eV or 10^{-23} J per particle. A temperature is therefore low for a given physical process when $k_B T$ is small compared to the characteristic energy of the process considered. Cryogenic temperatures thus reveal phenomena with low characteristic energy (Table 2), and enable their application when significantly lower than the characteristic energy of the phenomenon of interest. From Tables 1 and 2, it is clear that "low-temperature" superconductivity requires helium cryogenics: several examples of helium-cooled superconducting devices are shown in Figure 6. Considering vapour pressures of gases at low temperature (Figure 7), it is also clear that helium must be the working cryogen for achieving "clean" vacuum with cryopumps.

Table 2
Characteristic temperatures of low-energy phenomena

Phenomenon	Temperature [K]
Debye temperature of metals	few 100
High-temperature superconductors	~ 100
Low-temperature superconductors	~ 10
Intrinsic transport properties of metals	< 10
Cryopumping	few
Cosmic microwave background	2.7
Superfluid helium 4	2.2
Bolometers for cosmic radiation	< 1
Low-density atomic Bose-Einstein condensates	$\sim 10^{-6}$

## 2. CRYOGENIC FLUIDS

2.1 Thermophysical properties

The simplest way of cooling equipment with a cryogenic fluid is to make use of its latent heat of vaporization, e.g. by immersion in a bath of boiling liquid. As a consequence, the useful temperature range of cryogenic fluids is that in which there exists latent heat of vaporization, i.e. between the triple point and the critical point, with a particular interest in the normal boiling point, i.e. the saturation temperature at atmospheric pressure. This data is given in Table 1. In this introduction to cryogenics, we will concentrate on two cryogens: helium which is the only liquid at very low temperature, and nitrogen for its wide availability and ease of use for pre-cooling equipment and for thermal shielding.
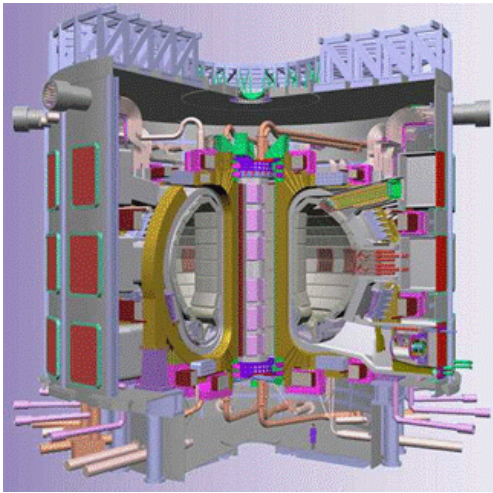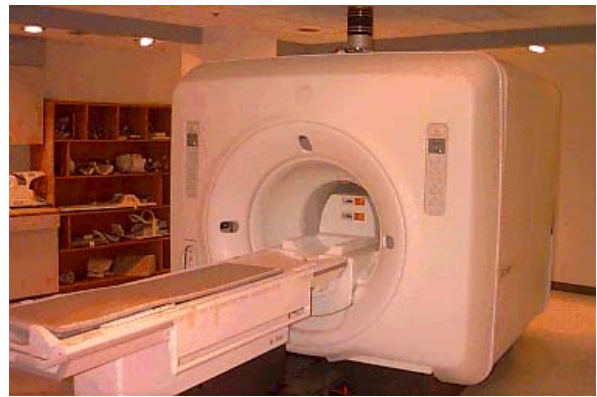
Figure 6 Helium-cooled superconducting devices a) Large Hadron Collider at CERN, b) 5 MW HTS ship propulsion motor (AMS), c) ITER experimental fusion reactor, d) whole-body MRI system (Bruker)
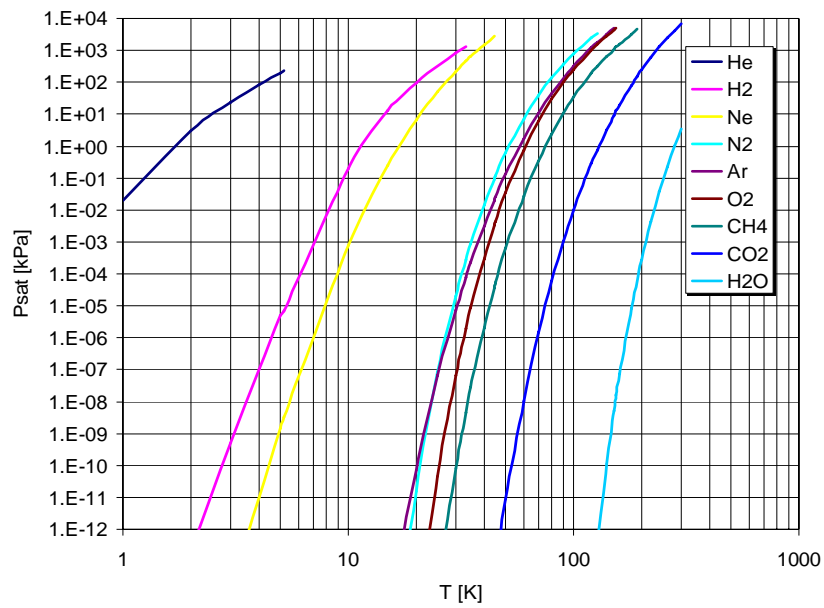

Figure 7 Vapour pressure of common gases at cryogenic temperature

To develop a feeling about properties of these cryogenic fluids, it is instructive to compare them with those of water (Table 3). In both cases, but particularly with helium, applications operate much closer to the critical point, i.e. in a domain where the difference between the liquid and vapour phases is much less marked: the ratio of liquid to vapour densities and the latent heat associated with the change of phase are much smaller. Due to the low values of its critical pressure and temperature, helium can be used as a cryogenic coolant beyond the critical point, in the supercritical state. It is also interesting to note that, while liquid nitrogen resembles water as concerns density and viscosity, liquid helium is much lighter and less viscous. This latter property makes it a medium of choice for permeating small channels inside superconducting magnet windings and thus stabilizing the superconductor.

Table 3
Properties of helium and nitrogen compared to water

Property	Helium	Nitrogen	Water
Normal boiling point [K]	4.2	77	373
Critical temperature [K]	5.2	126	647
Critical pressure [bar]	2.3	34	221
Liquid density* [kg/m^3]	125	808	960
Liquid/vapor density ratio*	7.4	175	1600
Heat of vaporization* [kJ/kg]	20.4	199	2260
Liquid viscosity* [µPl]	3.3	152	278

* at normal boiling point

2.2 Liquid boil-off

The factor of ten in latent heat of vaporization between helium and nitrogen, combined with the lower density of the former, induces a large difference in vaporization rates under the same applied heat load (Table 4). This illustrates the need for implementing much better insulation techniques in liquid helium vessels to achieve comparable holding times.

Table 4
Vaporization of liquid helium and liquid nitrogen at normal boiling point under 1 W applied heat load

Cryogen	[mg/s]	[l/h liquid]	[l/min gas NTP]
Helium	48	1.38	16.4
Nitrogen	5	0.02	0.24

Boil-off measurements constitute a practical method for measuring the heat load of a cryostat holding a saturated cryogen bath. In steady conditions, i.e. provided the liquid level in the bath is maintained constant, the boil-off $\dot{m}_{vap}$ precisely equals the vapor flow $\dot{m}_{out}$ escaping the cryostat, which can be warmed up to room temperature and measured in a conventional gas flow-meter. At decreasing liquid level though, part of the vapor will take the volume in the cryostat previously occupied by the liquid which has vaporized, and the escaping flow will be lower than the boil-off. More precisely, if the boil-off vapor is taken at saturation in equilibrium with the liquid

$$\dot{m}_{out} = \dot{m}_{vap}\left(1 - \frac{\rho_v}{\rho_l}\right) < \dot{m}_{vap} \tag{4}$$

The escaping gas flow measured must therefore be corrected upwards to obtain the true boil-off. From values of saturated liquid to vapor density ratios in Table 3, this correction factor is only 1.006 for nitrogen and can therefore be neglected. For helium though, it amounts to 1.16 and must clearly be taken into account.

2.3 Cryogen usage for equipment cooldown

For both fluids, the sensible heat of the vapour over the temperature range from liquid saturation to ambient is comparable to or larger than the latent heat of vaporization. This provides a valuable cooling potential at intermediate temperature, which can be used for thermal shielding or for pre-cooling of equipment from room temperature. The heat balance equation for cooling a mass of, say iron m_{Fe} of specific heat $C_{Fe}(T)$ at temperature T by vaporizing a mass dm of cryogenic liquid at saturation temperature T_v, latent heat of vaporization L_v and vapour specific heat C (taken as constant), is assuming perfect heat exchange with the liquid and the vapour

$$m_{Fe}\ C_{Fe}(T)\ dT = \ [L_v + C\ (T - T_v)]\ dm \tag{5}$$

Hence the specific liquid cryogen requirement for cool-down from temperature T_0

$$\frac{m}{m_{Fe}} = \int_{T_0}^{T} \frac{C_{Fe}(T)\,dT}{L_v + C\ (T - T_v)} \tag{6}$$

The term $C\ (T - T_v)$ adding to L_v in the denominator brings a strong attenuation to the specific liquid requirement, provided there is good heat exchange between the solid and the escaping vapor. Calculated values of specific liquid cryogen requirements for iron are given in Table 5, clearly demonstrating the interest of recovering the sensible heat of helium vapor, as well as that of pre-cooling equipment with liquid nitrogen.

Table 5
Volume [l] of liquid cryogens required to cool down 1 kg of iron

Using	Latent heat only	Latent heat and enthalpy of vapor
Liquid helium from 290 K to 4.2 K	29.5	0.75
Liquid helium from 77 K to 4.2 K	1.46	0.12
Liquid nitrogen from 290 K to 77 K	0.45	0.29

2.4 Phase domains

Typical operating domains with cryogenic helium are shown in Figure 8, superimposed on the – peculiar – phase diagram of the substance: the solid phase only exists under pressure and the normal liquid He I undergoes below 2.2 K a transition to another liquid phase, He II instead of solidifying. There is no latent heat associated with this phase transition, but a peak in the specific heat, the shape of which gave the name "λ-line" to the phase boundary. He II exhibits superfluidity, a macroscopic quantum behavior entailing very high thermal conductivity and very low viscosity. While operating in saturated He I provides fixed (saturation) temperature and high boiling heat transfer at moderate heat flux, it may develop instabilities in two-phase flow and is prone to boiling crisis above the peak nucleate boiling flux (about 1 W/cm^2). The use of mono-phase supercritical helium in forced-flow systems avoids the problems of two-phase flow. However, the strongly varying properties of the fluid in the vicinity of the critical point may create other issues, such as density wave oscillations. More fundamentally, supercritical helium exhibits no latent heat, so that applied heat loads result in temperature increases which must be contained by high flow-rate or periodic re-cooling in extended systems. At lower temperature, He II demonstrates excellent transport properties which make it a coolant of choice for advanced superconducting devices [3]. Besides the thermodynamic penalty of

lower temperature, the use of He II imposes that at least part of the cryogenic circuits operate at sub-atmospheric pressure, thus requiring efficient compression of low-pressure vapor and creating risks of dielectric breakdown and contamination by air in-leaks.

Thermo-physical properties of cryogenic fluids are available from tables, graphs and software running on personal computers, a selection of which is listed in the bibliography.
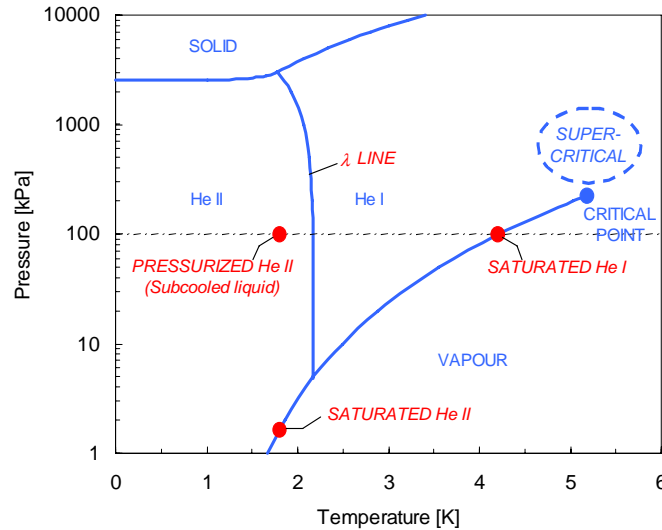

Figure 8 Phase diagram of helium, showing typical operating domains

3. HEAT TRANSFER AND THERMAL DESIGN

With the exception of superfluid helium, the heat transfer processes at work in cryogenics are basically the same as for any engineering temperature range. The strong variation of thermal properties of materials and fluids at low temperature however has two consequences: the relative and absolute magnitudes of the processes may be very different from those at room temperature, and the equations become non-linear, thus requiring numerical integration. Cryogenic thermal design is the art of using these processes adequately, either for achieving thermal insulation (cryostats, transfer lines) or for improving thermal coupling between equipment and coolant (cool-down & warm-up, thermal stabilization, thermometry) [4].

3.1 Solid conduction

Heat conduction in solids is represented by Fourier's law, expressing proportionality of heat flux with thermal gradient. In one dimension, this reads

$$Q = k(T)\, A\, \frac{\mathrm{d}T}{\mathrm{d}x} \tag{7}$$

This equation also defines the thermal conductivity $k(T)$ of the material, which varies with temperature. Conduction along a solid rod of length L, cross section A spanning a temperature range $[T_1, T_2]$, e.g. the support strut of a cryogenic vessel, is then given by the integral form

$$Q = \frac{A}{L} \int_{T_1}^{T_2} k(T)\, \mathrm{d}T \tag{8}$$

Thermal conductivity integrals $\int_{T_1}^{T_2} k(T)\, \mathrm{d}T$ of standard materials are tabulated in the literature. A few examples are given in Table 6, showing the large differences between good and bad thermal conducting materials, the strong decrease of conductivity at low temperatures, particularly for pure

metals, and the interest of thermal interception to reduce conductive heat in-leak in supports. As an example, the thermal conductivity integral of austenitic stainless steel from 80 K to vanishingly low temperature is nine times smaller than from 290 K, hence the benefit of providing a liquid nitrogen cooled heat sink on the supports of a liquid helium vessel. The lower thermal conductivity values of non-metallic composites, combined with their good mechanical properties, makes them materials of choice for low heat-inleak structural supports (Figure 9).

Table 6
Thermal conductivity integrals of selected materials [W/m]

From vanishingly low temperature up to	20 K	80 K	290 K
OFHC copper	11000	60600	152000
DHP copper	395	5890	46100
Aluminum 1100	2740	23300	72100
2024 aluminum alloy	160	2420	22900
AISI 304 stainless steel	16.3	349	3060
G-10 glass-epoxy composite	2	18	153

Figure 9 Non-metallic composite support post with heat intercepts for LHC superconducting magnets

3.2 Radiation

Blackbody radiation strongly and only depends on the temperature of the emitting body, with the maximum of the power spectrum given by Wien's law

$$\lambda_{max} \, T = 2898 \; [\mu m \; K] \tag{9}$$

and the total power radiated given by Stefan-Boltzmann's law

$$Q = \sigma A \, T^4 \tag{10}$$

with Stefan-Boltzmann's constant $\sigma \simeq 5.67 \; 10^{-8} \; W \; m^{-2} \; K^{-4}$. The dependence of the radiative heat flux on the fourth power of temperature makes a strong plea for radiation shielding of low-temperature vessels with one or several shields cooled by liquid nitrogen or cold helium vapor. Conversely, it makes it very difficult to cool equipment down to low temperature by radiation only: in spite of the 2.7 K background temperature of outer space (and notwithstanding the Sun's radiation and the Earth's albedo which can be avoided by proper attitude control), satellites or interplanetary probes can make use of passive radiators to release heat only down to about 100 K, and embarked active refrigerators are required to reach lower temperatures.

Technical radiating surfaces are usually described as "gray" bodies, characterized by an emissivity $\varepsilon < 1$

$$Q = \varepsilon \, \sigma A \, T^4 \tag{11}$$

The emissivity ε strictly depends on the material, surface finish, radiation wavelength and angle of incidence. For materials of technical interest, measured average values are found in the literature [5], a subset of which is given in Table 7. As a general rule, emissivity decreases at low temperature, for good electrical conductors and for polished surfaces. As Table 7 shows, a simple way to obtain this combination of properties is to wrap cold equipment with aluminum foil. Conversely, radiative thermal coupling requires emissivity as close as possible to that of a blackbody, which can be achieved in practice by special paint or adequate surface treatment, e.g. anodizing of aluminum.

Table 7
Emissivity of some technical materials at low temperature

	Radiation from 290 K, surface at 77 K	Radiation from 77 K, surface at 4.2 K
Stainless steel, as found	0.34	0.12
Stainless steel, mech. polished	0.12	0.07
Stainless steel, electro-polished	0.10	0.07
Stainless steel + aluminum foil	0.05	0.01
Aluminum, black anodized	0.95	0.75
Aluminum, as found	0.12	0.07
Aluminum, mech. polished	0.10	0.06
Aluminum, electro-polished	0.08	0.04
Copper, as found	0.12	0.06
Copper, mech. polished	0.06	0.02

The net heat flux between two "gray" surfaces at temperature T_1 and T_2 is similarly given by

$$Q = E \, \sigma A \, (T_1^{\,4} - T_2^{\,4}) \tag{12}$$

with the emissivity factor E being a function of the emissivities ε_1 and ε_2 of the surfaces, of the geometrical configuration and of the type of reflection (specular or diffuse) between the surfaces. Its precise determination can be quite tedious, apart from the few simple geometrical cases of flat plates, nested cylinders and nested spheres.

If an uncooled shield with the same emissivity factor E is inserted between the two surfaces, it will "float" at temperature T_S given by the energy balance equation

$$Q_s = E \, \sigma A \, (T_1^{\,4} - T_S^{\,4}) = E \, \sigma A \, (T_S^{\,4} - T_2^{\,4}) \tag{13}$$

Solving for T_S yields the value of $Q_s = Q / 2$: the heat flux is halved in presence of the floating shield. More generally, if n floating shields of equal emissivity factor are inserted between the two surfaces, the radiative heat flux is divided by $n + 1$.

3.3 Convection

The diversity and complexity of convection processes cannot be treated here. Fortunately, in the majority of cases, the correlations established for fluids at higher temperature are fully applicable to the cryogenic domain [6], and reference is made to the abundant technical literature on the subject. In

the case of forced convection, one should keep in mind that the high density and low viscosity of cryogenic fluids often result in flows with high Reynolds number Re and hence strong convection. The Nüsselt number $N\ddot{u}$ which characterizes the efficiency of convective heat transfer relative to conduction in the fluid, is an increasing function of the Prandtl Pr and Reynolds numbers, respectively representing the ratio of mass to heat transport, and the ratio of inertial to viscous forces

$$N\ddot{u} = \mathrm{f}\,(Pr, Re) \tag{14}$$

The case of natural convection at low temperature however deserves particular mention, as this mechanism, usually weak at room temperature except on very large scales, becomes dominant in cryogenic equipment. In this case, the Nüsselt number is an increasing function of the Prandtl and Grashof Gr numbers, with the latter representing the ratio of buoyancy to viscous forces

$$N\ddot{u} = \mathrm{f}\,(Pr, Gr) \tag{15}$$

For gases, while Pr is about constant and independent of temperature, Gr is proportional to the heated volume, temperature difference and coefficient of volume thermal expansion which scales as $1/T$ in the ideal case. As a consequence, there may exist in helium cryostats strong natural convection processes with Grashof numbers up to the 10^{12} range, i.e. higher than those encountered in the general circulation of the Earth's atmosphere. This has been used by hydrodynamics specialists to study turbulent convection in extreme conditions. The cryogenic engineer sees it as a powerful mechanism for cooling equipment and homogenizing its temperature.

3.4 Gas conduction

Since J. Dewar's invention (1898) of the cryogenic vessel which bears his name, evacuated envelopes provide the best insulation against heat transport in gaseous media. At low pressure, convection becomes negligible and only residual gas conduction is at work. This process operates in two distinct regimes, depending upon the value of the mean free path of gas molecules ℓ relative to the typical distance d between the cold and warm surfaces.

The mean free path of gas molecules, as predicted by kinetic theory, scales with the square root of temperature and inversely with pressure and the square root of molar mass. It therefore becomes large at low pressure, high temperature and for light gas species.

When $\ell \ll d$ corresponding to higher residual pressure, the probability of interaction of a given molecule with others before it travels distance d is high (viscous regime), and heat diffuses as in any continuous medium

$$Q = k(T)\,A\,\frac{\mathrm{d}T}{\mathrm{d}x} \tag{16}$$

Note that the thermal conductivity $k(T)$ of the gas is independent of pressure.

When $\ell \gg d$ at low residual pressure, the molecular regime prevails and the heat transfer between two surfaces at temperatures T_1 and T_2 is given by Kennard's law

$$Q = A\,\alpha(T)\,\Omega\,P\,(T_2 - T_1) \tag{17}$$

where Ω is a parameter depending upon the gas species, and α is the "accommodation coefficient" representing the thermalisation of molecules on the surfaces; its value depends on T_1, T_2, the gas species and the geometry of the facing surfaces. Note that the conductive heat flux in molecular regime is proportional to pressure P and independent of the spacing between the surfaces (and therefore not amenable to the concept of thermal conductivity). Typical values of heat flux by gas conduction at cryogenic temperature are given in Table 8.

Table 8
Typical values of heat flux to vanishingly low temperature between flat plates [W/m^2]

Black-body radiation from 290 K	401
Black-body radiation from 80 K	2.3
Gas conduction (100 mPa helium) from 290 K	19
Gas conduction (1 mPa helium) from 290 K	0.19
Gas conduction (100 mPa helium) from 80 K	6.8
Gas conduction (1 mPa helium) from 80 K	0.07
MLI (30 layers) from 290 K, pressure < 1 mPa	1-1.5
MLI (10 layers) from 80 K, pressure < 1 mPa	0.05
MLI (10 layers) from 80 K, pressure 100 mPa	1-2

3.5 Multi-layer insulation

Multi-layer insulation (MLI) is based on multiple reflecting shields wrapped around the cryogenic piece of equipment to be insulated, with the aim of benefiting from the $n + 1$ reduction factor in radiative heat in-leak. In practice, this is implemented in the form of aluminum or aluminized polymer films, with low packing density achieved by crinkling or by insertion of a net-type spacer between layers. The wrapping can be made by winding the layers and spacer *in situ*, or by pre-fabricated blankets installed and held in place by insulating fasteners (Figure 10). In all cases, MLI is a complex thermal system, involving the combination of radiation, solid-contact conduction, and residual-gas conduction between layers. As a result, increasing the number of layers, while beneficial for cutting radiation, usually results in increased packing with more contacts and trapped residual gas between layers, two effects which increase heat transfer. In view of the non-linearity of these elementary processes, thermal optimization requires layer-to-layer modeling and efficient control of the critical parameters. In practice, performance is measured on test samples and measured data is available from an abundant literature. Typical values for some practical MLI systems are given in Table 8.

Figure 10 Prefabricated MLI blankets being installed around an accelerator superconducting magnet

Of particular interest is the case of operation in degraded vacuum, where the heat in-leak by molecular conduction is directly proportional to the residual pressure. The presence of a multilayer system which segments the insulation space into many cells thermally in series significantly contains the increase in heat in-leak to the low-temperature surface (Table 8). In this respect, the multilayer system is no longer used for its radiative properties, but for the reduction of molecular gas conduction.

In the extreme case of complete loss of vacuum in a liquid helium vessel, MLI also efficiently limits the heat flux which would otherwise be very high due to condensation of air on the cold wall, thus alleviating the requirements for emergency discharge systems.

3.6 Vapor-cooling of necks and supports

The enthalpy of cryogen vapor escaping from a liquid bath can be used to continuously intercept conduction heat along solid supports and necks connecting the cryogenic bath with the room temperature environment (Figure 11).
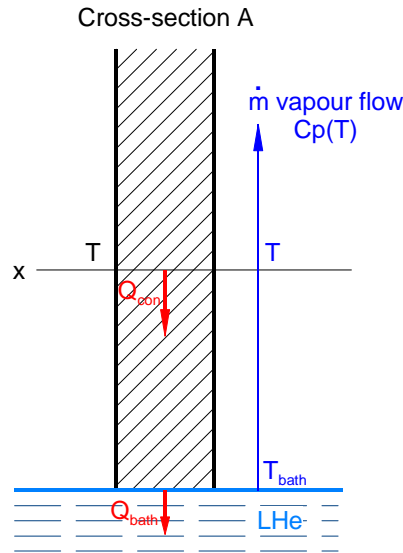
Figure 11 Vapour cooling of necks and supports with perfect heat exchange

Assuming steady state and perfect heat exchange between the escaping vapor and the solid, the energy balance equation reads

$$k(T)\, A \frac{\mathrm{d}T}{\mathrm{d}x} = Q_v + \dot{m}\, C\,(T - T_v) \tag{18}$$

where Q_v is the heat reaching the liquid bath and $\dot{m}$ is the vapor mass flow-rate. In the particular case of self-sustained vapor cooling, i.e. when the vapor mass flow-rate $\dot{m}$ precisely equals the boil-off from the liquid bath,

$$Q_v = L_v\, \dot{m} \tag{19}$$

Combining equations (18) and (19) and integrating yields the value of Q_v

$$Q_v = \frac{A}{L} \int_{T_v}^{T0} \frac{k(T)}{1 + (T - T_v)\dfrac{C}{L_v}}\, \mathrm{d}T \tag{20}$$

The denominator of the integrand clearly acts as an attenuation term for the conduction integral. Numerical results for helium and a few materials of technical interest appear in Table 9. If properly used, the cooling power of the vapor brings an attenuation of one to two orders of magnitude in the conductive heat in-leak.

Table 9

Attenuation of heat conduction between 290 K and 4 K by self-sustained helium vapor cooling [W/cm]

Material	Purely conductive regime	Self-sustained vapor cooling
ETP copper	1620	128
OFHC copper	1520	110
Aluminum 1100	728	39.9
Nickel 99% pure	213	8.65
Constantan	51.6	1.94
AISI 300 stainless steel	30.6	0.92

Vapor cooling can also be used for continuous interception of other heat loads than solid conduction. In cryogenic storage and transport vessels with vapor-cooled shields, it lowers shield temperature and thus reduces radiative heat in-leak to the liquid bath. In vapor-cooled current leads, a large fraction of the resistive power dissipation by Joule heating is taken by the vapor flow, in order to minimize the residual heat reaching the liquid bath [7].

A worked-out example of how these diverse thermal insulation techniques are implemented in a real design is given in reference [8].

4. REFRIGERATION AND LIQUEFACTION

Refrigeration and liquefaction of gases are historically at the root of cryogenics, as they constitute the enabling technology which gave access to the low-temperature domain. They have developed over the years along several lines, to become a specialized subject which would deserve a thorough presentation. In the following, we shall briefly describe the basic thermodynamics, the cooling processes at work and the corresponding equipment in the case of helium refrigerators/liquefiers based on the Claude cycle. For a more complete review, see reference [9].

4.1 Thermodynamics of refrigeration

A refrigerator is a machine raising heat Q_i from a low-temperature source T_i to a higher-temperature sink (usually room temperature) T_0, by absorbing mechanical work W_i; doing so, it rejects heat Q_0 (see Figure 12). These quantities are related through the application of the first (Joule) and second (Clausius) principles of thermodynamics

$$Q_0 = Q_i + W_i \tag{21}$$

$$\frac{Q_0}{T_0} \geq \frac{Q_i}{T_i} \tag{22}$$

In equation (22), the equality applies to the case of reversible process. From the above

$$W_i \geq T_0 \frac{Q_i}{T_i} - Q_i \tag{23}$$

This expression can be written in three different ways. Introducing the reversible entropy variation $\Delta S_i = Q_i/T_i$

$$W_i \geq T_0 \Delta S_i - Q_i \tag{24a}$$

Another form isolates the group $(T_0/T_i - 1)$ as the proportionality factor between Q_i and W_i, i.e. the minimum specific refrigeration work

14

$$W_i \geq Q_i\left(\frac{T_0}{T_i} - 1\right) \tag{24b}$$

As Carnot has shown in 1824, this minimum work can only be achieved through a cycle constituted of two isothermal and two adiabatic transforms (Carnot cycle). All other thermodynamic cycles entail higher refrigeration work for the same refrigeration duty.

A third form of equation (23) is

$$W_i \geq \Delta E_i \tag{24c}$$

This introduces the variation of exergy $\Delta E_i = Q_i (T_0/T_i - 1)$, a thermodynamic function representing the maximum mechanical work content (Gouy's "énergie utilisable") of a heat quantity Q_i at temperature T_i, given an environment at temperature T_0 .
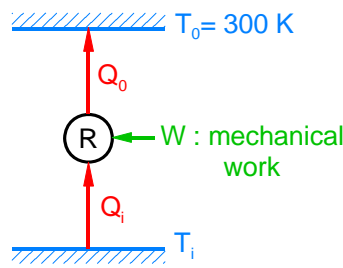
Figure 12 Thermodynamic scheme of a refrigerator

Equation (24b) enables to calculate the minimum mechanical power needed to extract 1 W at 4.5 K (saturated liquid helium temperature at 1.3 bar pressure, i.e. slightly above atmospheric) and reject it at 300 K (room temperature), yielding a value of 65.7 W. This is the power that would be absorbed by a refrigerator operating on a Carnot cycle between 4.5 K and 300 K. In practice, the best practical cryogenic helium refrigerators have an efficiency of about 30 % with respect to a Carnot refrigerator, hence a specific refrigeration work of about 220.

Cryogenic refrigerators are often required to provide cooling duties at several temperatures or in several temperature ranges, e.g. for thermal shields or continuous heat interception (see paragraph 3.6 above). Equation (24b) can then be applied to the cooling duty at every temperature and every elementary mechanical power W_i summed or integrated in the case of continuous cooling. This also allows comparison of different cooling duties in terms of required mechanical work.

4.2 Helium refrigerators vs. liquefiers

A 4.5 K helium refrigerator absorbs heat isothermally at this temperature, usually by re-condensing cold helium vapor at saturation (saturation pressure 1.3 bar). By contrast, a liquefier also eventually condenses cold helium vapor at saturation, but starting from gaseous helium at 300 K which it must first pre-cool to 4.5 K (Figure 13). From equation (24a), the minimum mechanical power for helium liquefaction is

$$W_{liq} = W_{condens} + W_{precool} \tag{25}$$

$$W_{liq} = T_0 \Delta S_{condens} - Q_{condens} + T_0 \Delta S_{precool} - Q_{precool} \tag{26}$$

The heat quantities $Q_{condens}$ and $Q_{precool}$ exchanged at constant pressure are given by the enthalpy variations $\Delta H_{condens}$ and $\Delta H_{precool}$. With $T_0 = 300$ K and the entropy and enthalpy differences taken from thermodynamic tables, one finds $W_{liq} = 6628$ W per g/s of helium liquefied. Given the minimum specific mechanical work of 65.7 at 4.5 K, this yields an approximate equivalence of about 100 W at 4.5 K for 1 g/s liquefaction. More precisely, a liquefier producing 1 g/s liquid helium at 4.5 K will absorb the same power (and thus have similar size) as a refrigerator extracting about 100 W at 4.5 K, provided they both have the same efficiency with respect to the Carnot cycle. For machines with mixed refrigeration and liquefaction duties, this equivalence can be approximately verified by trading some liquefaction against refrigeration around the design point and *vice versa*.
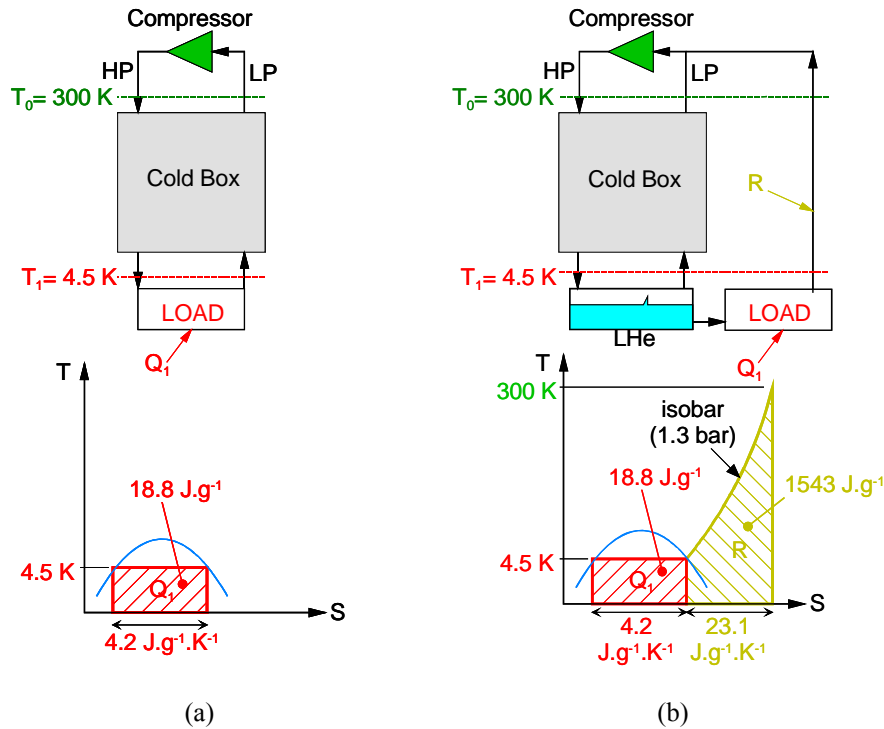
Figure 13 Helium refrigerator (a) vs. liquefier (b)

4.3 Real cycles and refrigeration equipment

So far we have only addressed cryogenic refrigeration and liquefaction through thermodynamics, i.e. through the exchanges of mass, heat and work at the boundaries of machines seen as "black boxes". We will now consider cycles, cooling methods and equipment of real refrigerators.

In order to minimize the specific mechanical work requirement (and hence the size and power consumption), an efficient refrigerator should try and approximate the Carnot cycle, which is represented by a rectangle on the temperature-entropy diagram: the two isotherms are horizontal lines, while the two isentropic transforms are vertical lines. To liquefy helium, the base of the rectangle should intercept the liquid-vapor dome (Figure 14).

However, superimposing this cycle on the temperature-entropy diagram of helium shows that one should operate at a high pressure of about 613 kbar (!), with a first isentropic compression from 1.3 bar to 82 kbar (!), followed by an isothermal compression. This is clearly impractical, and real helium cycles are elongated along isobar (or isochoric) lines, thus involving transforms which require heat exchange between the high- and low-pressure streams. This heat exchange can be performed in recuperative or regenerative heat exchangers, respectively for continuous or alternating flows. In the following, we focus on the continuous-flow cycles using recuperative heat exchangers which constitute the operating principles of large-capacity helium refrigerators and liquefiers.
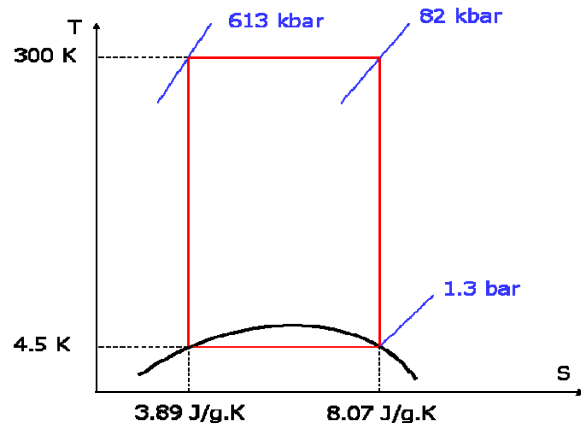
Figure 14 A hypothetical Carnot cycle for helium liquefaction

Practical elementary cooling processes are shown on the temperature-entropy diagram in Figure 15. The gas stream can first undergo quasi-isobar cooling in a counter-flow heat exchanger (segment AB_1): modern refrigerators make use of brazed aluminum plate heat exchangers (Figure 16). Refrigeration can be produced by adiabatic (quasi-isentropic) expansion with extraction of mechanical work (segment AB'_2): the expansion engine is a gas turbine, with the extracted power transmitted to a compressor wheel sharing a common shaft and later dissipated in a brake circuit (Figure 17). A third process is isenthalpic Joule-Thomson expansion, i.e. without extraction of mechanical work, in a valve or restriction (segment AB_3).

Unfortunately, this latter process does not does work for ideal gases, the enthalpy of which is a sole function of temperature. For real gases, however, enthalpy depends both on temperature and pressure, so that isenthalpic expansion can produce warming or cooling, depending upon the slope of the isenthalps on the diagram. In order to cool the gas stream, Joule-Thomson expansion must start below a limit called the inversion temperature. The values of inversion temperature for cryogenic fluids (Table 10) show that while air can be cooled from room temperature by Joule-Thomson expansion (the risk of freezing the pressure reducer on the air bottle is well known to scuba divers), helium must first be pre-cooled down to below its inversion temperature of 43 K. The moderate downward slope of isenthalps on the temperature-entropy diagram indicates that in any case, Joule-Thomson expansion generates substantial entropy. Its relative inefficiency with respect to adiabatic expansion is however accepted in view of the simplicity of its implementation, particularly when it results in partial condensation of the stream entailing two-phase flow conditions which would be difficult to handle in an expansion turbine.

Table 10
Maximum values of Joule-Thomson inversion temperature

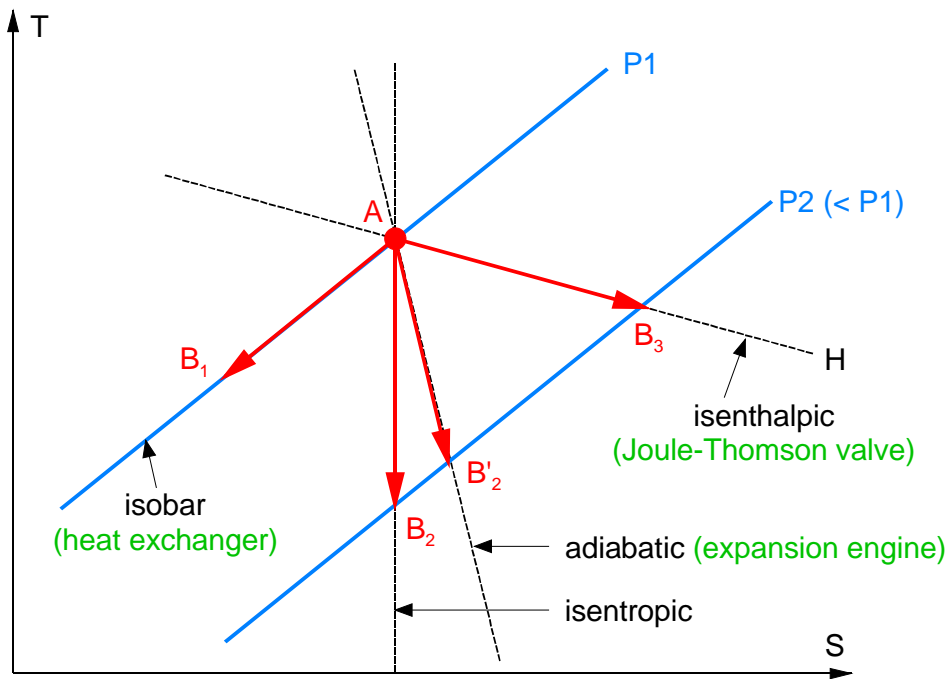| Cryogen	Maximum inversion temperature [K]
Helium	43
Hydrogen	202
Neon	260
Air	603
Nitrogen	623
Oxygen	761

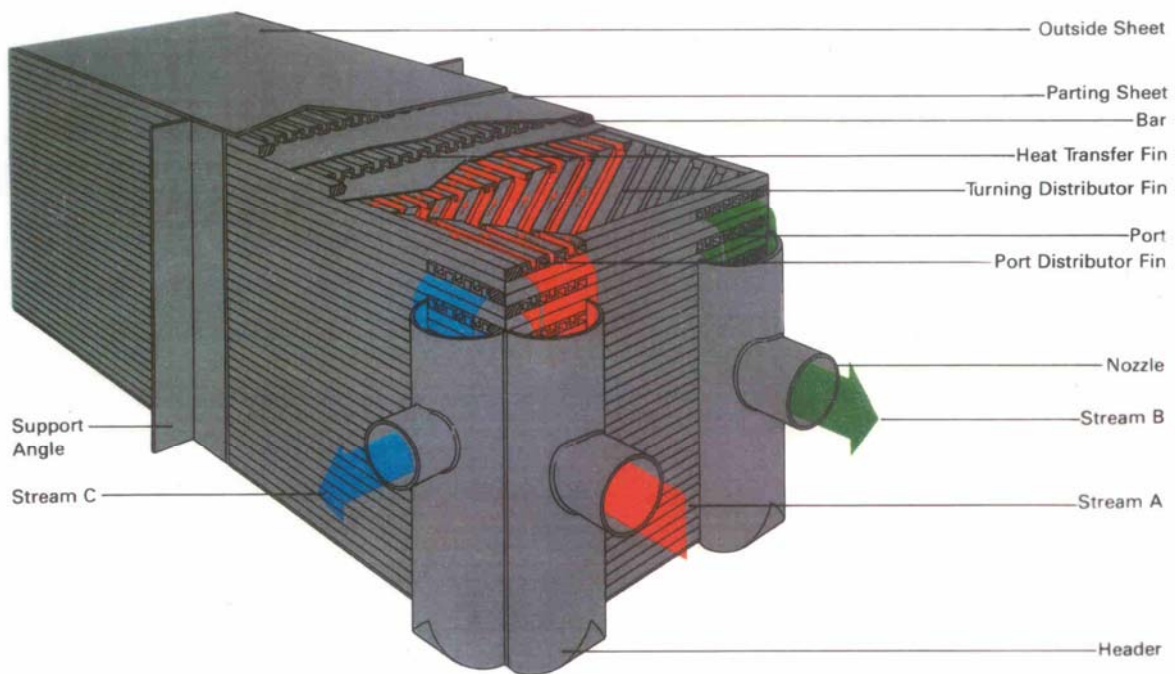Figure 15 Elementary cooling processes shown on temperature-entropy diagram

Figure 16 Schematic view of a brazed aluminium plate heat exchanger
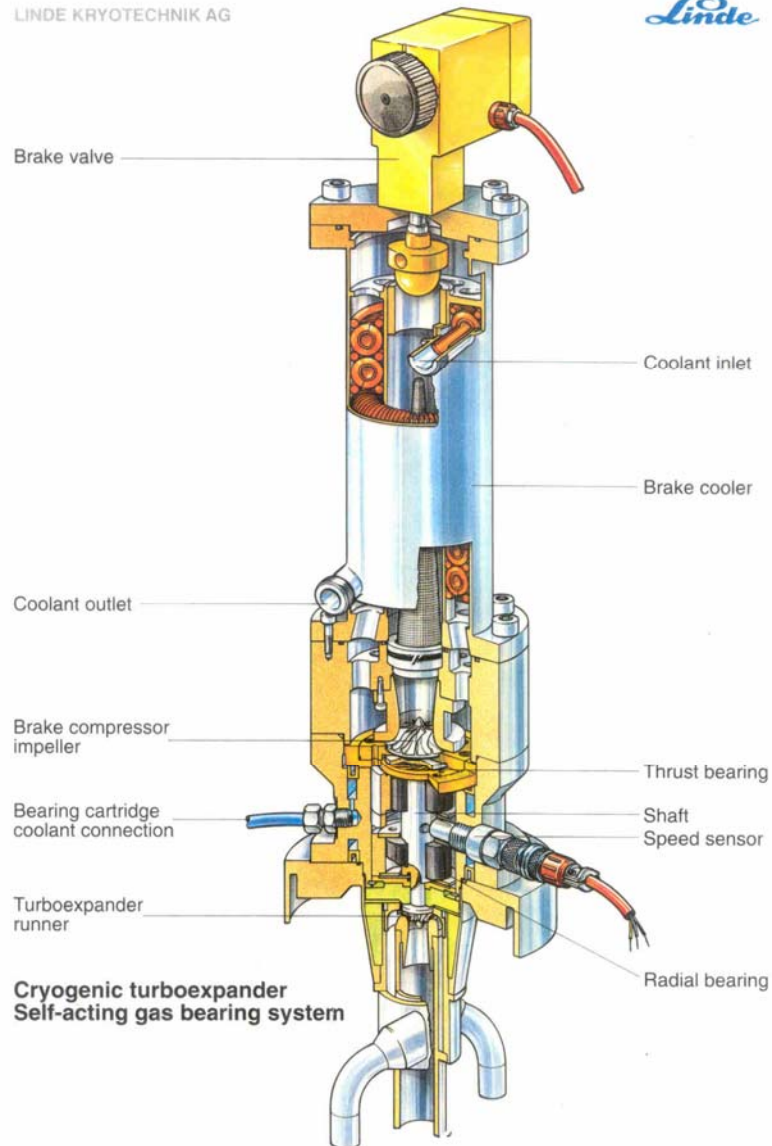
Figure 17 Cryogenic turbo-expander (source Linde)

These elementary cooling processes are combined in practical cycles, a common example for helium refrigeration is provided by the Claude cycle and its refinements. A schematic two-pressure, two-stage Claude cycle is shown in Figure 18: gaseous helium, compressed to HP in a lubricated screw compressor, is re-cooled to room temperature in water-coolers, dried and purified from oil aerosols down to the ppm level, before being sent to the HP side of the heat exchange line where it is refrigerated by heat exchange with the counter-flow of cold gas returning on the LP side. Part of the flow is tapped from the HP line and expanded in the turbines before escaping to the LP line. At the bottom of the heat exchange line, the remaining HP flow is expanded in a Joule-Thomson valve and partially liquefied.
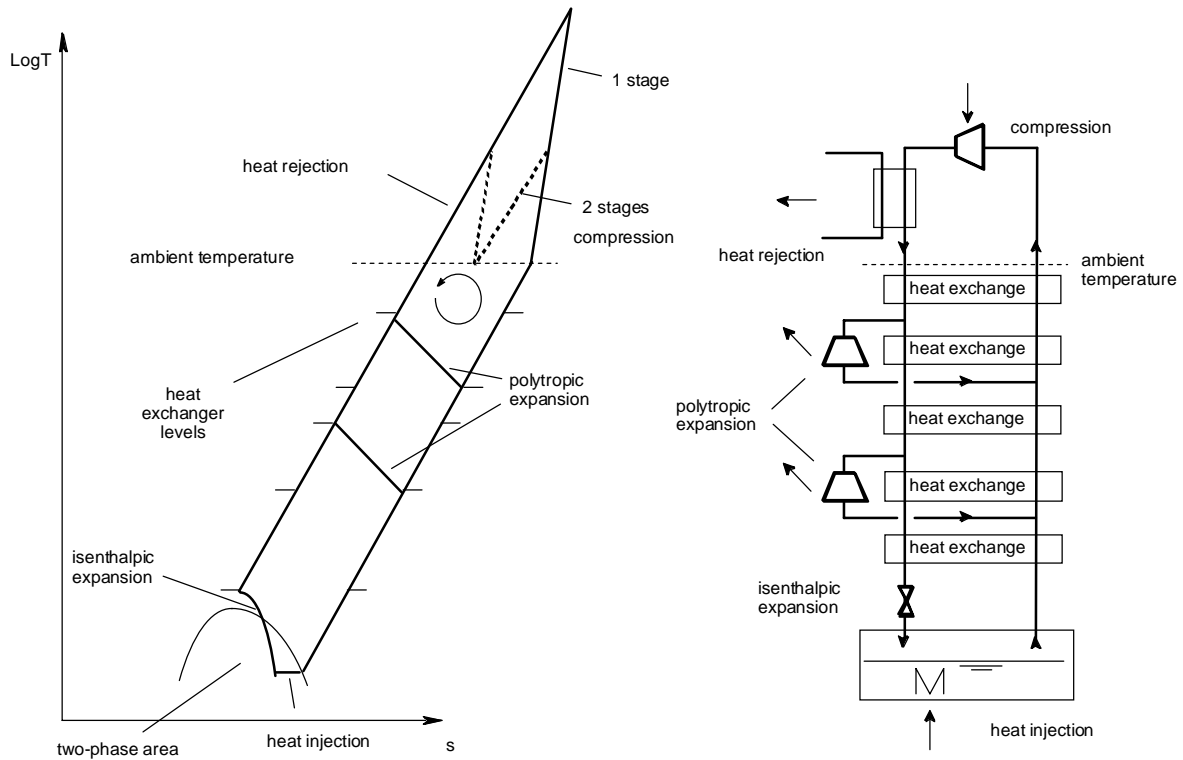
Figure 18 Schematic example of two-pressure, two-stage Claude cycle: T-S diagram (left) and flow scheme (right)

Large-capacity helium refrigerators and liquefiers operate under this principle, however with many refinements aiming at meeting specific cooling duties and improving efficiency and flexibility of operation, such as three- and sometimes four-pressure cycles, liquid nitrogen pre-cooling of the helium stream, numerous heat exchangers, many turbines in series or parallel arrangements, Joule-Thomson expansion replaced by adiabatic expansion in a "wet" turbine, cold compressors to lower the refrigeration temperature below 4.5 K. A view of such a large plant appears in Figure 19.

The capital cost of these complex machines is high, but scales less than linearly with refrigeration power, which favors large units. Operating costs are dominated by that of electrical energy, typically amounting to about ten percent of the capital cost per year in case of quasi-continuous operation. For overall economy, it is therefore very important to seek high efficiency, which is also easier to achieve on large units. For a review of these aspects, see reference [10].

5. CONCLUSION

This brief paper has presented the basic ideas and principles of the most important aspects of cryogenics, i.e. cryogenic fluids, heat transfer, thermal design and refrigeration. It has also provided the reader with typical numerical values of the relevant parameters, enabling him to perform order-of-magnitude estimates and apply his engineering judgement. There is of course much more to say on each of these topics, some of which have significantly developed over the years and still constitute areas of technical progress. Many other subjects not addressed here also pertain to cryogenic engineering, such as materials at low temperature, storage, handling and transfer of fluids, two-phase flow and discharge, vacuum and leak-tightness technology, instrumentation (in particular thermometry), process control, impurity control and safety. In all cases, the interested reader is referred to the selected bibliography for detailed information and to the proceedings of the cryogenic engineering conferences for recent developments.

a) Compressor station

b) Coldbox

Figure 19 18 kW @ 4.5 K helium refrigerator for the LHC at CERN

ACKNOWLEDGEMENTS

SELECTED BIBLIOGRAPHY

Introduction to low temperatures

K. Mendelssohn, The quest for absolute zero, 2nd edition, Taylor & Francis, London (1977).

J. Wilks & D.S. Betts, An introduction to liquid helium, 2nd edition, Oxford Science Publications, Clarendon Press, Oxford (1987).

R.G. Scurlock (ed.), History and origins of cryogenics, Clarendon Press, Oxford (1992).

Ph. Lebrun, Cryogenics, key to advanced science and technology, Bulletin of the IIR, Paris, LXXXIII 2003-6 (2003) 4, http://www.iifiir.org/2enarticles_bull03_6.pdf.

Cryogenic engineering textbooks

R.B. Scott, Cryogenic engineering, Van Nostrand, Princeton (1959).

R.R. Conte, Eléments de cryogénie, Masson, Paris (1970).

G.G. Haselden, Cryogenic fundamentals, Academic Press, London (1971).

R.A. Barron, Cryogenic systems, Oxford University Press, New York (1985).

B.A. Hands, Cryogenic engineering, Academic Press, London (1986).

S.W. van Sciver, Helium cryogenics, Plenum Press, New York (1989).

K.D. Timmerhaus & T.M. Flynn, Cryogenic process engineering, Plenum Press, New York (1989).

Fluid and material properties

R.D. Mc Carty, Thermodynamic properties of helium 4 from 2 to 1500 K at pressures to 10^8 Pa, J. Chem. Phys. Ref. Data, 2 (1973) 923.

W.C. Reynolds, Thermodynamic properties in SI: graphs, tables and computational equations for 40 substances, Department of Mechanical Engineering, Stanford University (1979).

Cryogenic properties of materials, NIST Cryogenic Technologies Group, www.cryogenics.nist.gov

V. Arp, HEPAK, Thermophysical properties of helium, www.cryodata.com

R.D. Mc Carty, GASPAK, Thermophysical properties of 36 fluids, www.cryodata.com

Conference proceedings

Proceedings of the Cryogenic Engineering Conferences (CEC) and International Cryogenic Material Conferences (ICMC), *in* Advances in Cryogenic Engineering (multiple publishers).

Proceedings of the International Cryogenic Engineering Conferences (ICEC) (multiple publishers).

CERN Accelerator School proceedings

S. Turner (ed,), Proceedings of the CAS "Superconductivity in particle accelerators", Hamburg, CERN 89-04, Geneva (1989).

S. Turner (ed.), Proceedings of the CAS "Superconductivity in particle accelerators", Hamburg, CERN 96-03, Geneva (1996).

S. Russenschuck & G. Vandoni (eds.), Proceedings of the CAS "Superconductivity and cryogenics for accelerators and detectors", Erice, CERN-2004-008, Geneva (2004).

REFERENCES

[1] Oxford English Dictionary, 2nd edition, Oxford University Press (1989).

[2] New International Dictionary of Refrigeration, 3rd edition, IIR-IIF Paris (1975).

[3] Ph. Lebrun & L. Tavian, The technology of superfluid helium, CERN-2004-008, Geneva (2004) 375.

[4] G. Vandoni, Heat transfer, CERN-2004-008, Geneva (2004) 325.

[5] W. Obert *et al.*, Emissivity measurements of metallic surfaces used in cryogenic applications, Adv. Cryo. Eng. 27 (1982) 293.

[6] M.C. Jones & V. Arp, Review of hydrodynamics and heat transfer for large helium cooling systems, *in* Advances in refrigeration at the lowest temperatures, IIR-IIF Commission A1-2, Zürich (1978) 41.

[7] Yu.L. Buyanov, Current leads for use in cryogenic devices, principle of design and formulae for design calculations, Cryogenics 25 (1985) 94.

[8] Ph. Lebrun, Design of a cryostat for superconducting accelerator magnets: the LHC main dipole case, CERN-2004-008, Geneva (2004) 348.

[9] U. Wagner, Refrigeration, CERN-2004-008, Geneva (2004) 295.

[10] S. Claudet *et al.*, Economics of large helium cryogenic systems: experience from recent projects at CERN, Adv. Cryo. Eng. 45B (2000) 1301.